MASS SPECTRUM OF THE 1385 MeV $\Lambda^0+\pi^0$ RESONANCE FROM 1.5 GeV/c π^- MESONS ON PROTONS (*)

C. T. Coffin, L. J. Curtis, D. I. Meyer, and K. M. Terwilliger
University of Michigan, Ann Arbor, Mich.

(presented by K. M. Terwilliger)

We have investigated the reaction

$$1.5\ \text{GeV/c}\ \pi^- + p \rightarrow \Lambda^0 + K^0 + \pi^0$$

in a spark chamber experiment at the Cosmotron. Our preliminary results show the Y_1^* resonance at 1385 MeV and are consistent with it having a spin of 1/2.

The experimental arrangement is shown in Fig. 1. The incoming 1.5 GeV/c pions pass through two beam defining counters and a small spark chamber and into a 1″ liquid hydrogen target. The target is followed by an anticoincidence counter, the main spark chamber, then a coincidence counter. The counter system triggers the spark chambers when an interaction of the pion in the hydrogen target produces just neutral secondaries, one or more of which decay in the main spark chamber. The chamber electrodes are made of 1 mil Al foil to minimize neutron and gamma ray conversions.

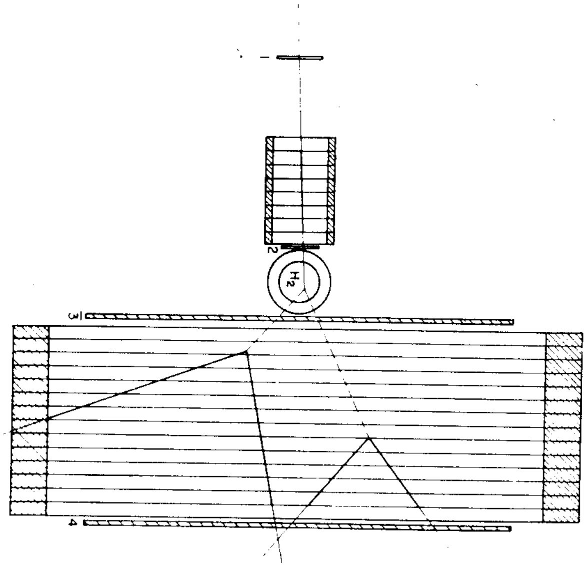

Fig. 1 Experimental arrangement. π^- incident from the top produces a Λ^0 and K^0 which decay in the spark chamber. Counters 1, 2 and 4 are in coincidence and $\bar{3}$ is in anticoincidence to trigger the chambers on events of this type.

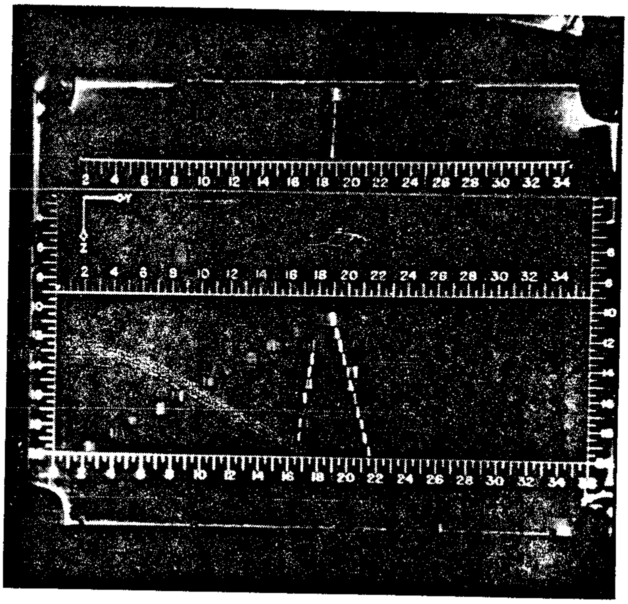

Fig. 2 Photograph of an associated production event. The geometry is the same as in Fig. 1. The units of the reticle are cm.

A photograph of one view of an event is shown in Fig. 2. The beam is incident from the top; the track of the incoming pion in the small spark chamber can

---

(*) This work is supported by the U.S. Atomic Energy Commission.

be seen above the top reticle. The hydrogen target is just below between the two reticles, and the main spark chamber is approximately outlined by the lower rectangle of reticles. Four views of each event were photographed on one frame: two views at right angles for measurement, the other two at smaller angles to help resolve ambiguities in identification.

The position of the event origin is determined by extending the decay planes of the V's back through the incoming pion track. The event origin and the decay origins and opening angles determine the kinematics of the reaction, even without a magnetic field, although there are far fewer checks than there would be with a field. The event is calculated two ways, assuming first one track is the K^0, then the other. There is usually no doubt as to the correct channel. The choice is confirmed by examination of the spark densities, which are a fairly good measure of the relative particle velocities.

The criteria that the event origins be consistent with being inside the hydrogen target (not more than one standard deviation outside) and that the kinematics check within an amount determined by looking at events which were certainly within the target, eliminates practically all the background (hydrogen out) events. The mass resolution of the experiment, with this criteria, can be seen in a histogram of the missing mass X^0 in the reaction 1.5 GeV/c $\pi^- + p \to K^0 + X^0$ as shown in Fig. 3. About 40% of all the data is used in this plot. Just 12 of these events are expected to be background, spread uniformly from 1000 MeV to 1430 MeV. The positions of the centres of the λ^0 and Σ^0 peaks are below the accepted values by about 5 MeV, which is consistent with the accuracy of our hot wire measurements of the central momentum of the pion beam. The full width at half maximum of both peaks is 40 MeV. The dependence of the X^0 mass on angular errors is about three times as large in the Λ^0 and Σ^0 region as it is near the Y_1^{*0}; at the Y_1^{*0} the net experimental resolution curve, due to angle errors and beam momentum errors, is estimated to have a width of about 15 MeV.

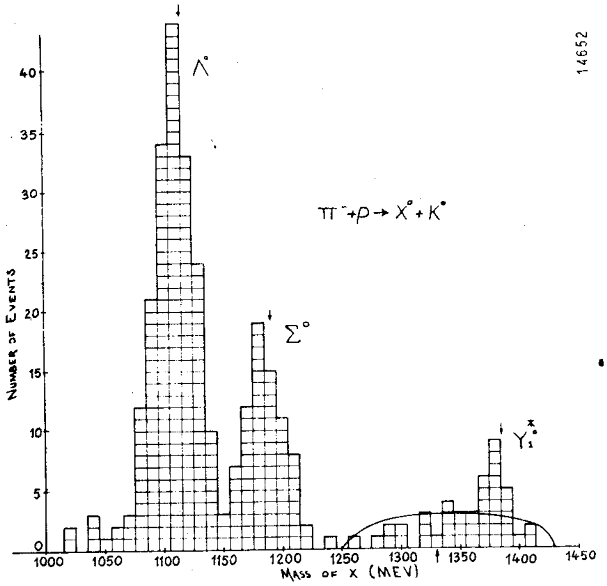

Fig. 3 Histogram of the missing mass X^0 in the reaction 1.5 GeV/c $\pi^- + p \to X^0 + K^0$. The arrows at the top of the peaks refer to the accepted values of the particle masses. The 3 body phase space plot in the Y^* region is normalized to the total number of events there.

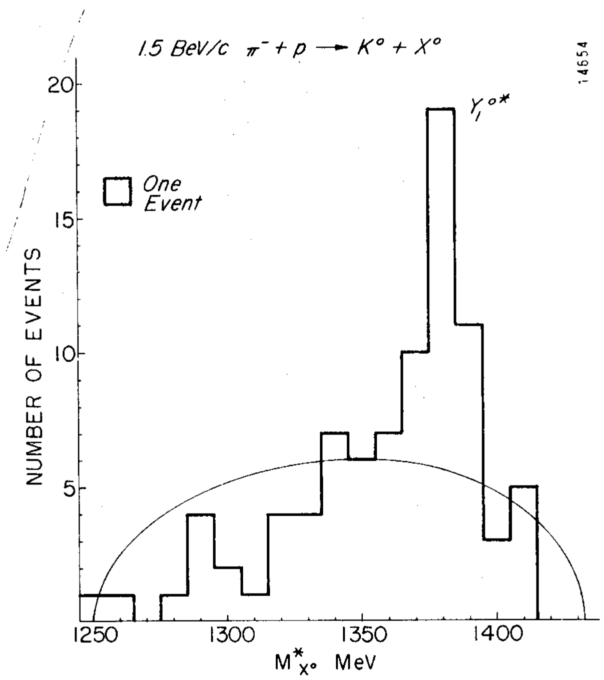

Fig. 4 Histogram of the missing mass X^0 in the region 1250 MeV to 1430 MeV. A 3 body phase space plot is also shown.

A histogram of the mass spectrum in the $\Lambda^0 + \pi^0$ region, for K^0 production angles $0{,}5 < \cos \theta_{KCM} < 1$, with almost all our data, 135 events, is shown in Fig. 4. Included are approximately 12 background events, again randomly distributed. The beam momentum has been corrected to 1.508 GeV/c from the Λ^0 results. The Y_1^* resonance shows up strongly with its maximum in agreement with the 1385 MeV value obtained in previous Y_1^* experiments. The width of the peak, with the experimental resolution removed appears to be about 25 MeV. Measurement accuracies are such that any given event may be due to $\Sigma^0 K^0 \pi^0$ production rather than $\Lambda^0 K^0 \pi^0$. However an examination of the spectrum of the missing mass in the reaction $X^0 \rightarrow \Lambda^0 +$ neutrals indicates that the fraction of $\Sigma^0 K^0 \pi^0$ events is probably not large.

We have assumed that the events in the region $1360 < M_{Y*} < 1410$ are Y_1^* (85 events) and have examined their decay. Neither an Adair plot, Λ-π, or a Λ-K distribution show significant forward-backward asymmetry, consistent with a lack of large final state interactions. A folded Adair distribution is shown in Fig. 5. It is consistent with a spin of 1/2 for the Y_1^*. The cosine of the Y_{CM}^* production angle is restricted to the region 0.4→1.0 to reduce the number of reactions where $\Delta m_l \neq 0$, so that the Adair analysis would apply. The momentum of the Y^* in the production CM was chosen low for this experiment, 190 MeV/c, to improve the probability that the production of $\Delta m_2 \neq 0$ is small, for the same reason. However, our production angular distributions are not fully analyzed and no statement can be made about the actual fraction of events in which $\Delta m_l \neq 0$.

The decay of the Y_1^{*0} with respect to the production normal is consistent with up-down symmetry. The distribution is presented folded in Fig. 6. It is also flat, consistent with spin 1/2, but again not proving it, for the Y_1^* may be produced unpolarized.

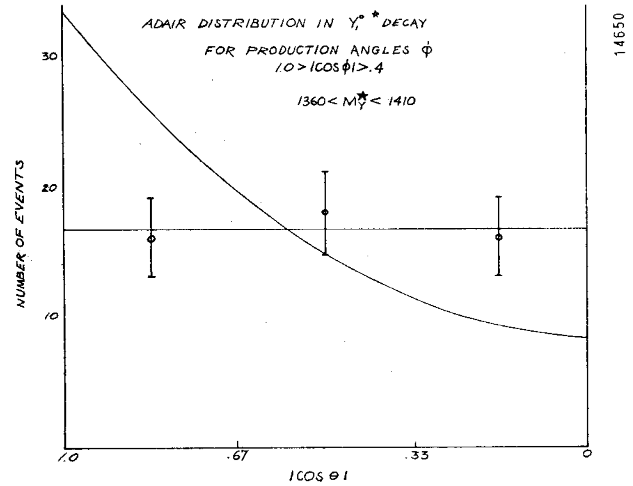

Fig. 5 Adair distribution in Y_1^{0*} decay, along with the curves expected for spin 1/2 and spin 3/2 particles.

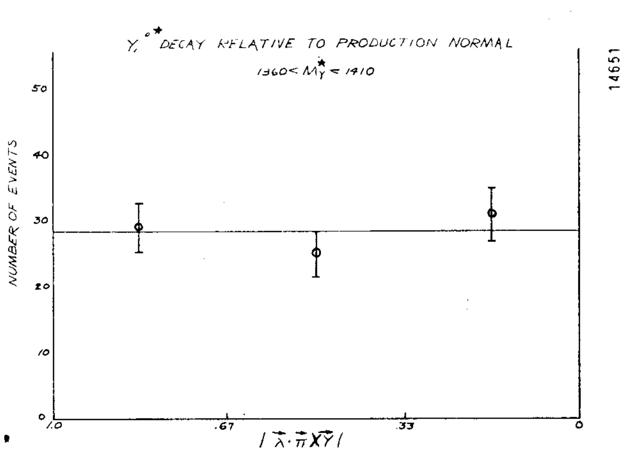

Fig. 6 Y_1^{0*} decay distribution relative to the production normal.